

High-dynamic range compressive spectral imaging by adaptive filtering

Nelson Diaz

Department of Computer and
Informatics Engineering,
Universidad Industrial de Santander,
Bucaramanga, Colombia 680002.
Email: nelson.diaz@correo.uis.edu.co

Hoover Rueda

Department of Electrical and
Computer Engineering,
University of Delaware,
Newark, DE, 19716, USA.
Email: rueda@udel.edu

Henry Arguello

Department of Computer and
Informatics Engineering,
Universidad Industrial de Santander,
Bucaramanga, Colombia 680002.
Email: henarfu@uis.edu.co

Abstract—Compressive hyperspectral imaging systems (CSI) capture the three-dimensional (3D) information of a scene by measuring two dimensional (2D) using a small set of coded focal plane array (FPA) compressive measurement. A reconstruction algorithm takes advantage of the compressive measurements sparsity to recover the 3D data cube. Traditionally, CASSI uses block-unblock coded apertures to spatially modulate the light, the modulation has binary entries. In CASSI the quality of the reconstructed images depends on the design of these coded apertures and the FPA saturation. This work presents a new CASSI architecture based on grayscale coded apertures (GCA) which reduce the saturation and increase the dynamic range of the FPA detector. The set of codes is calculated in a realtime adaptive manner such that the FPA compressive measurements are used to determine the structure of the GCA. Simulations show the improvement in the quality of the reconstructed images of the architecture based on GCA.

Keywords—Compressive sensing, hyperspectral imaging, saturation, dynamic range, coded aperture, optical imaging.

I. INTRODUCTION

The Coded Aperture Snapshot Spectral Imaging System (CASSI) is an imaging architecture which senses the three dimensional spatio-spectral information of a scene with a single two dimensional (2D) coded random projection measurement set [1]. The CASSI optical architecture comprises five optical elements: an object lens is used to form an image of a scene in the plane of the coded aperture; the coded aperture modulates the spatial information over the complete wavelength range; a relay lens transmits the coded light field onto a dispersive element, the dispersive element disperses the light before it impinges on the focal plane array (FPA), the FPA captures the compressive measurements. Given a set of compressive measurements, compressive sensing theory (CS) [2], [3], [4] is used to reconstruct the underlying data cube of size $N \times N \times L$ from just $N \times (N + (L - 1))$ measurements, where N and N are the spatial dimensions and L is the spectral depth of the data cube. The quality of reconstructed images relies on the design of the 2D set of coded apertures which block-unblock the light from the scene.

A single shot CASSI measurement may not provide sufficient number of compressive measurements. A recent modification in CASSI allows multi-shot sensing procedures which increase the number of compressive measurements, [5], [6].

In this architecture, each shot uses a distinct coded aperture that remains fixed during the integration time of the detector [5], [6]. The quality of reconstructed images improves in multi-shot CASSI in proportion to the number of compressive measurements [7], [8]. Each CASSI measurement shot adds simultaneously $N(N + L - 1)$ compressive measurements. The total number of available measurement with K shots is therefore $KN(N + L - 1)$.

Traditionally, block-unblock coded apertures are implemented using piezo systems [9] or a digital-micromirror-device (DMD) [10] to vary the coding pattern in each snapshot. The disadvantage of block-unblock coded apertures is that they have just two binary values and therefore reduce the dynamic range of the FPA sensor. To address this limitation, we propose the use of GCA which can be implemented using a DMD or other block-unblock device with high switching rate. DMD takes advantage of the fast switching time of the micro-mirrors which enables the use of a pulsewidth modulation technique for the production of grayscale values. GCA have been used to obtain spectral images with selective spectral profile using the CASSI optical system [11]. GCA can be used to yield a modulation of the transmittance and to increase the dynamic range of the reconstructions.

Saturation occurs in the detector when compressive measurements exceed the dynamic range of the quantizer. In that case, these measurements take the value of the saturation level [12]. In CASSI and multi-shot CASSI, each saturated pixel in the sensor induces errors in the reconstructed image. Typically, CASSI system employs CCD or CMOS sensor, both affected by saturation depending on their dynamic range.

This work extends the compressive capabilities of CASSI by replacing the traditional block-unblock coded apertures by a set of GCA. Figure 1(a) shows the detail of the grayscale-adaptive coded aperture where the attenuated pixel represents an oscillating spatial modulator. Figure 1(b) shows the sketch of the proposed architecture. Grayscale-adaptive coded aperture multi-shot CASSI is motivated by the possibility to reduce saturation levels through modulation of the amplitude of the incoming scene. So we propose the use of an adaptive filter (AF) which updates the GCA between shots. The AF compute the next GCA based on previous compressive measurement and prior GCA to reduce the positions of the scene that contribute to saturation.

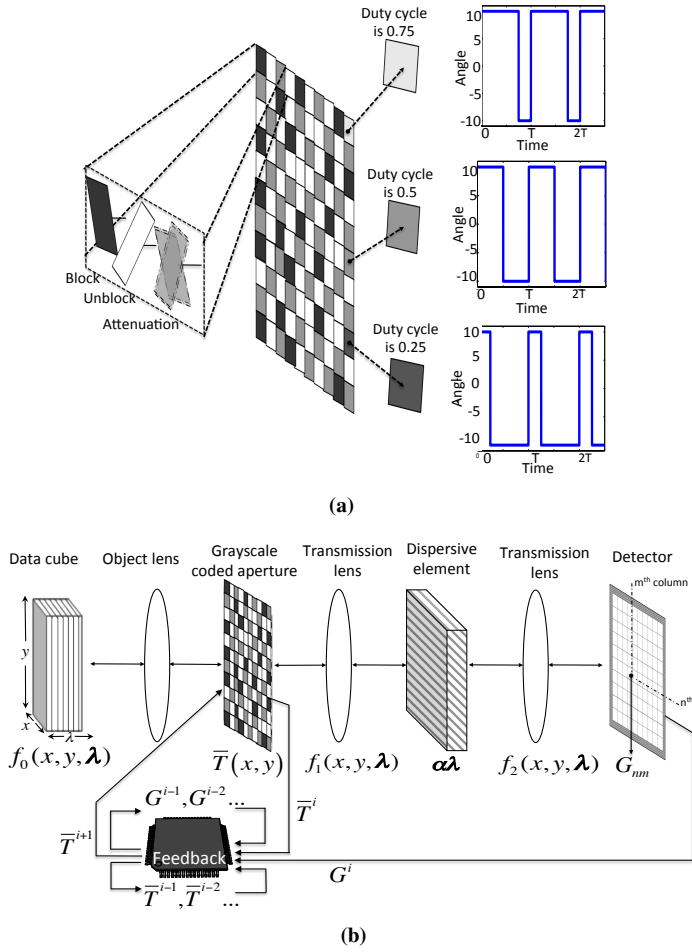


Fig. 1: (a) Illustration of a grayscale coded aperture (GCA) (b) Sketch of the GCA-based CASSI system with adaptive filtering to reduce the sensing saturation. The feedback process uses the current measurement and the previous GCAs to create the next GCA to be used.

In the following we introduce the block-unblock CASSI optical model and present the grayscale-adaptive-based model. Simulations are performed to evaluate the improvements attained by the proposed grayscale-adaptive coded apertures.

II. SYSTEM MODEL

A. Block-Unblock CASSI System Model

The coded aperture single shot spectral imaging system uses a traditional block-unblock coded aperture $T(x, y)$ to modulate the spatio-spectral density $f_0(x, y, \lambda)$, where (x, y) are the spatial dimensions and λ represents the spectral dimension. The resulting coded field $f_1(x, y, \lambda)$, is then dispersed by the dispersive element, resulting in,

$$f_2(x, y, \lambda) = \iint T(x', y') f_0(x', y', \lambda) \times h(x - x' - \alpha\lambda, y - y') dx' dy', \quad (1)$$

where $T(x', y')$ is the transmission function representing the coded aperture, $h(x - x' - \alpha\lambda, y - y')$ is the optical impulse

response of the system and $\alpha\lambda$ is the dispersion induced by the dispersive element assuming linear dispersion. The compressive measurements across the FPA are realized by the integration of the field $f_2(x, y, \lambda)$ over the detector range sensitivity. The spectral density in front of the detector is given by $g(x, y) = \int_{\Lambda} f_2(x, y, \lambda) d\lambda$. When the optical impulse response of the system is assumed linear and ideal, the resulting spectral density is

$$g(x, y) = \int f_0(x + \alpha\lambda, y, \lambda) T(x + \alpha\lambda, y) d\lambda. \quad (2)$$

The coded aperture $T(x, y)$ can be represented as a spatially pixelated array. Assuming the coded aperture pixel size is Δ_t and $t_{n', m'}$ represent a binary value, (0) block and (1) unblock, the coded aperture can be expressed as,

$$T(x, y) = \sum_{n', m'} t_{n', m'} \text{rect} \left(\frac{x}{\Delta_t} - m', \frac{y}{\Delta_t} - n' \right). \quad (3)$$

Representing the spatio-spectral source density being integrated on the sensor in discrete form as $F_{n', m', k}$ such that $n' \in \{0, \dots, N-1\}$ indexes the x -axis, $m' \in \{0, \dots, N-1\}$ the y -axis and $k \in \{0, \dots, L-1\}$ the wavelength, Eq. 2 can be succinctly expressed as,

$$G_{n, m} = \sum_{k=0}^{L-1} F_{(n-k), m, k} T_{(n-k), m} + \omega_{n, m}, \quad (4)$$

where $G_{n, m}$ is the intensity at the $(n, m)^{th}$ position of the detector \mathbf{G} with dimensions $(N + L - 1) \times N$, for $n \in \{0, \dots, (N + L - 1)\}$, and $m \in \{0, \dots, N - 1\}$. The spectral data cube F has size $N \times N \times L$, and the indexes $(n - k)$ is defined between $1 \leq (n - k) \leq N$, $T_{n, m}$ is the $(n, m)^{th}$ value in the spatial modulator and ω represents the noise of the system.

B. Grayscale CASSI System Model

In this paper the block-unblock coded aperture is replaced with a GCA, which modulates the source along the spatial coordinates. The CASSI system architecture with GCA is illustrated in Fig. 1(b), where the traditional block-unblock coded aperture is replaced by the GCA depicted in Fig. 1(a). The coding is now realized by the GCA represented by $\hat{T}(x, y)$ which is applied to the spatio-spectral density source $f_0(x, y, \lambda)$, resulting in the coded field $f_1(x, y, \lambda)$. This coded field differs from the one achieved with the block-unblock coded aperture in that a particular element of the grayscale code attenuates the wavelengths instead of blocking or unblocking the complete spectrum at a given spatial location. The entries of the coded aperture $t_{n', m'} = \{0, \dots, l-1\}$, being l the number of grayscale levels of the spatial modulator. In this way, Eq. 4 can be rewritten as,

$$G_{n, m} = \sum_{k=0}^{L-1} F_{(n-k), m, k} \hat{T}_{(n-k), m} + \omega_{n, m}. \quad (5)$$

C. FPA Saturation in CASSI

Saturation occurs when the measurements exceed the dynamic range of the sensor quantizer. The quantizer has finite dynamic range due to two reasons, the first is related to physical limitations that allow a finite range voltage to be correctly converted to bits, and the second is that only a finite number of bits are available to represent each value. Quantization with saturation is referred to as finite-range quantization [12]. The errors imposed by finite-range quantization are unbounded. Compressive sensing (CS) recovery techniques only provide guarantees for noise that is bounded, or bounded with high probability [12]. There exist some reconstruction algorithms that try to correct saturation by software [12], [14], [15]. In contrast, we propose the saturation correction in the sensing stage, in a real-time manner. Dealing with saturation is important in CASSI because it reduces the attainable reconstruction quality. Figure 2 shows examples of compressive measurements saturated by three distinct percentages of saturated pixels (0%, 5% and 10%, respectively), and their corresponding attained reconstructions using 4 shots. Notice that, the higher the saturation percentages, the lower the quality of the reconstructed images.

D. Adaptive Estimation of the GCA

In order to reduce the saturation level from the compressive snapshots, an adaptive filter (AF) is designed such that it adaptively attenuate the entries of the spatial modulator when they contribute to saturation. The process is considered adaptive because either the previous coded apertures and the current compressive snapshot are considered the inputs to compute the attenuated coded apertures for the next snapshot as is illustrated in Fig. 1(b). The input source is attenuated before it is integrated by the detector, consequently, these coded apertures will exhibit non-integer values, thus generating what we call GCA. Formally, let \mathbf{V}^i be the i^{th} weight matrix, where $i \in \{1, \dots, K\}$, whose entries $V_{n,m}^i$ measure how many times the coded aperture entry $T_{n,m}^i$ contribute to saturate entries in the sensor. In particular, the entries of \mathbf{V}^i can be written as

$$V_{n,m}^i = \sum_{\ell=n-(L-1)}^n u[G_{\ell,m}^i - s] + 1, \quad (6)$$

where $u[\cdot]$ is the Unit step function, $G_{\ell,m}^i$ is the $(\ell, m)^{\text{th}}$ pixel from the i^{th} compressive snapshot; $s = 2^b - 1$ represents the saturation level of the sensor, which depends on the number of bits (b) of the sensor, 1 is added in Eq. 6 because when $\sum_{\ell=n-(L-1)}^n u[G_{\ell,m}^i - s] = 0$ then $V_{n,m}^i = 1$ attenuates only the coded apertures entries that contribute to saturation. Notice that Eq. 6 can be easily calculated in a real time approach because each $V_{n,m}^i$ is a counter computed from compressive measurements \mathbf{G} with $V_{n,m}^i \in \{1, \dots, L + 1\}$. Based on the weighted matrix, a heuristic penalization function is generated by assuming that the attenuation in a pixel of the spatial modulator is inversely proportional to the weight matrix \mathbf{V} . That is, the penalization function can be seen as the attenuation matrix \mathbf{W} whose entries W_{nm}^i are given by,

$$W_{n,m}^i = \left(\frac{1}{V_{n,m}^i} \right) \cdot \left(\frac{1}{V_{n,m}^{i-1}} \right), \quad (7)$$

where \mathbf{V}^0 and \mathbf{V}^1 are assumed to be all-ones matrix. Notice that the attenuation matrix \mathbf{W}^i takes into account the previous weighted matrices as means of the memory in the adaptive filter to consider the information from previous snapshots. Given the K randomly generated block-unblock coded apertures $\mathbf{T}^1, \dots, \mathbf{T}^K$, the corresponding GCAs $\hat{\mathbf{T}}^1, \dots, \hat{\mathbf{T}}^K$ are generated according to,

$$\hat{\mathbf{T}}^{i+1} = \mathbf{T}^{i+1} \circ \mathbf{W}^i, \quad (8)$$

where $\mathbf{A} \circ \mathbf{B}$ is the Hadamard product between matrices \mathbf{A} and \mathbf{B} . Notice that $\hat{\mathbf{T}}^1 = \mathbf{T}^1$, that is, the first GCA remains as the original, since the adaptive filter needs feedback to calculate a new GCA, the feedback only occurs after the first snapshot.

III. SPECTRAL IMAGE RECONSTRUCTION

Compressive sensing theory can be used to recover a spatio-spectral signal $\mathbf{f} \in \mathbb{R}^{N \times N \times L}$ or its vector representation $\mathbf{f} \in \mathbb{R}^{N \cdot N \cdot L}$. Let $\boldsymbol{\theta}$ be a S -sparse representation of \mathbf{f} in some basis $\boldsymbol{\Psi}$, such that $\mathbf{f} = \boldsymbol{\Psi}\boldsymbol{\theta}$ can be approximated by a linear combination of S vectors of $\boldsymbol{\Psi}$ with $S \ll (N \cdot N \cdot L)$. Then, \mathbf{f} can be reconstructed from d random projections with high probability when $d \gtrsim S \log(N \cdot N \cdot L) \ll (N \cdot N \cdot L)$. In CASSI the projected measurements can be represented in matrix form, such that $\mathbf{y} = \mathbf{H}\mathbf{f}$, where \mathbf{H} is a $(N(N + L - 1) \times (N \cdot N \cdot L))$ matrix whose structure is determined by the coded apertures and the dispersive element. Similarly, multi-shot CASSI is represented as $\mathbf{y}^\ell = \mathbf{H}^\ell \mathbf{f}$, where \mathbf{H}^ℓ represents the effect of the ℓ^{th} coded aperture [7], [8]. The set of K compressive measurements with a distinct coded aperture is then assembled as $\mathbf{y} = [(\mathbf{y}^0)^T, \dots, (\mathbf{y}^{K-1})^T]^T$. The CASSI projections can be represented alternatively as $\mathbf{y} = \mathbf{H}\boldsymbol{\Psi}\boldsymbol{\theta}$, where the matrix $\mathbf{A} = \mathbf{H}\boldsymbol{\Psi}$ is the sensing matrix. The reconstructed data cube can be obtained by solving the minimization problem $\mathbf{f} = \boldsymbol{\Psi}(\arg\min_{\boldsymbol{\theta}} \|\mathbf{y} - \mathbf{H}\boldsymbol{\Psi}\boldsymbol{\theta}\|_2 + \tau\|\boldsymbol{\theta}\|_1)$ where

$\mathbf{H} = [(\mathbf{H}^0)^T, \dots, (\mathbf{H}^{K-1})^T]^T$, $\boldsymbol{\theta}$ is a S -sparse representation of \mathbf{f} on the basis $\boldsymbol{\Psi}$, and τ is a constant of regularization. The compressive sensing reconstruction is realized using the GPSR algorithm [13]. The basis representation $\boldsymbol{\Psi}$ is set to be

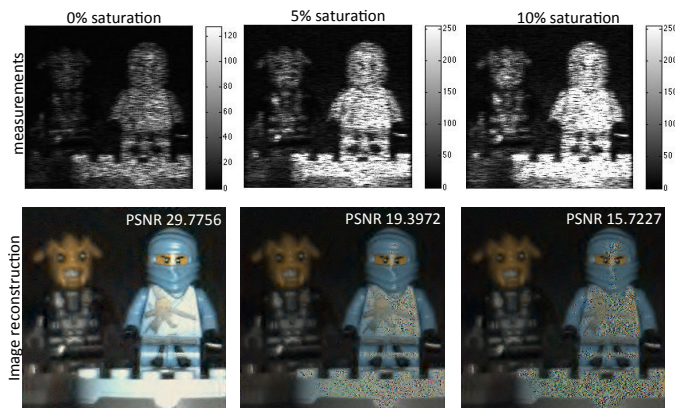


Fig. 2: Compressive measurements with 3 different levels of saturation and their respective reconstructions. (First row) Compressive measurements with 0%, 5%, and 10% of pixels saturated. (Second row) The corresponding reconstructions for 0%, 5%, and 10% of saturation using 4 shots.

the Kronecker product of two basis $\Psi = \Psi_1 \otimes \Psi_2$, where Ψ_1 playing the role of spatial sparsifier is the 2D-Wavelet Symmlet 8 basis and Ψ_2 being the spectral sparsifier is the 1D-DCT basis.

IV. RESULTS

In this section the grayscale-adaptive CASSI system is compared against the traditional CASSI with block-unblock coded apertures. A set of compressive measurements are simulated using the models in Eq. (4) and Eq. (5). The test data cube \mathbf{F} with 256×256 pixels of spatial resolution and $L = 8$ spectral bands is shown in Fig. 3. The measurements were constructed using a test spectral database obtained using a wide-band Xenon lamp as the light source, and a visible monochromator which spans the spectral range between 450nm and 650nm. The image intensity was captured using a CCD camera exhibiting 256×256 pixels.

The simulations are performed in a desktop architecture with an Intel i7-4770 3.4Ghz processor, 32 GB of RAM memory and using Matlab R2012b. The block-unblock coded apertures entries are realizations of a Bernoulli random variable such that the transmittance of each pattern is constant, 25%. The GPSR algorithm use a value $\tau = 0.0001$. The GCA are random realizations of block, unblock and attenuation elements, such that the transmittance in the first shot is 25% and, it is updated in the following shots by the adaptive filter. The number of saturated pixels in the measurements is varied from 0% to 10%. The coded apertures are designed to have 256×256 spatial resolution.

Figure 4 shows four snapshots using the block-unblock and the grayscale-adaptive coded apertures. The higher the snapshot number the lower the percentage of saturation in the compressive measurements. In addition, when more than four snapshots are captured, the percentage of saturation is approximately 0%. The silhouette of the compressive saturated measurements can be observed in the grayscale-adaptive coded aperture after the first snapshot. The resulting silhouette occurs when the weighted matrix attenuates the pixels in the coded aperture which are responsible for saturated values in the compressive measurements.

Figure 5 shows the average reconstruction PSNR as a function of the percentage of saturation. The grayscale adaptive and the block-unblock coded apertures are compared for two, four, six, and eight snapshots. In both cases there were included tests with noise, in which the measurements were affected with Gaussian noise with SNR = 10 dB.



Fig. 3: Spectral datacube for experimental simulations.

Figure 6 shows the average PSNR of the reconstructed data cubes as a function of the number of snapshots. The recon-

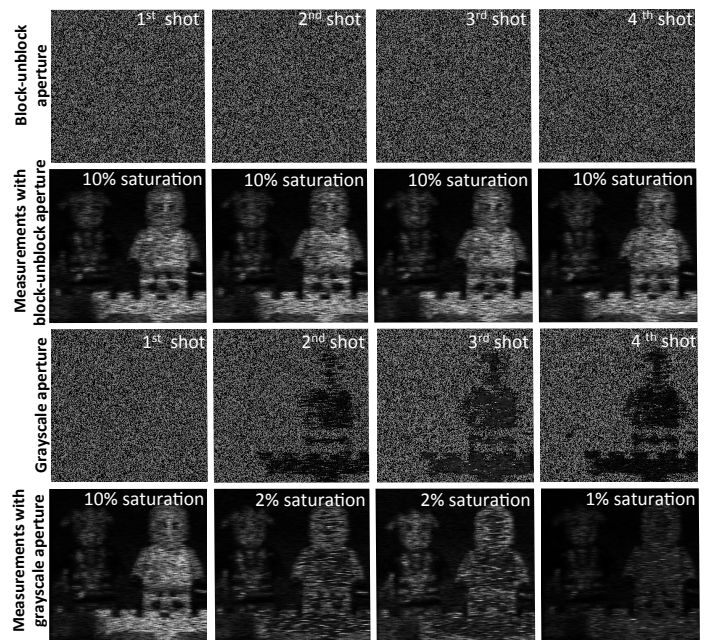


Fig. 4: Comparison between block-unblock and grayscale-adaptive coded apertures for four shots. The block-unblock and the grayscale-adaptive coded apertures and the corresponding compressive measurements are shown. Notice that saturation decrease between snapshots for GCA.

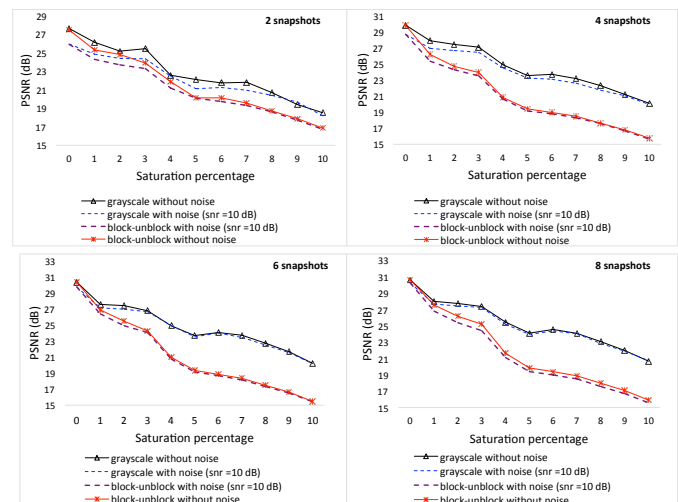


Fig. 5: Average reconstructions PSNR as a function of the percentage of saturation. The grayscale adaptive coded apertures are compared with block-unblock coded apertures. The PSNR is measured for GCA and block-unblock coded apertures for percentages of saturation between 1% and 10%.

structed datacubes were obtained from FPA measurements with saturation levels of 1%, 4%, 7% and 10%, respectively. The block-unblock coded apertures and the GCAs are compared adding Gaussian noise with SNR = 10 dB. The Fig. 7 shows the reconstruction with block-unblock which attains 15.4032 dB, and with grayscale-adaptive coded aperture attaining 27.5215 dB. The two reconstructions were obtained from FPA measurements with 10% of saturated pixels.

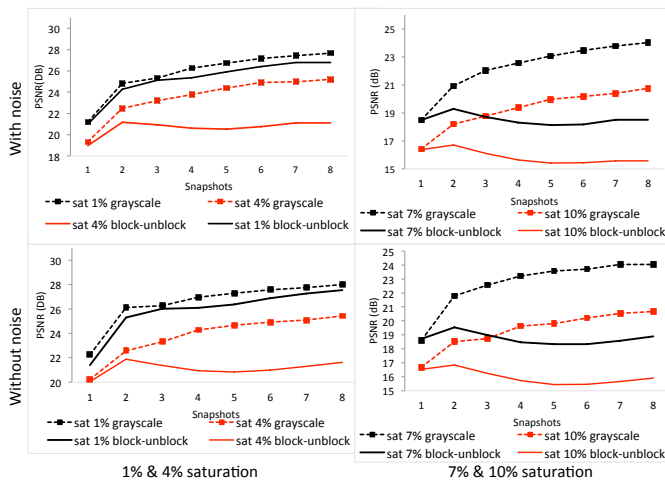


Fig. 6: Average PSNR of the reconstructed data cubes as a function of measurement snapshots. The block-unblock-based and the grayscale adaptive-based CASSI imagers are compared at distinct percentage of saturation. (top-left) 1% and 4% of saturation with noise (top-right) 7% and 10% of saturation with noise (bottom-left) 1% and 4% of saturation without noise and (bottom-right) 7% and 10% of saturation without noise.

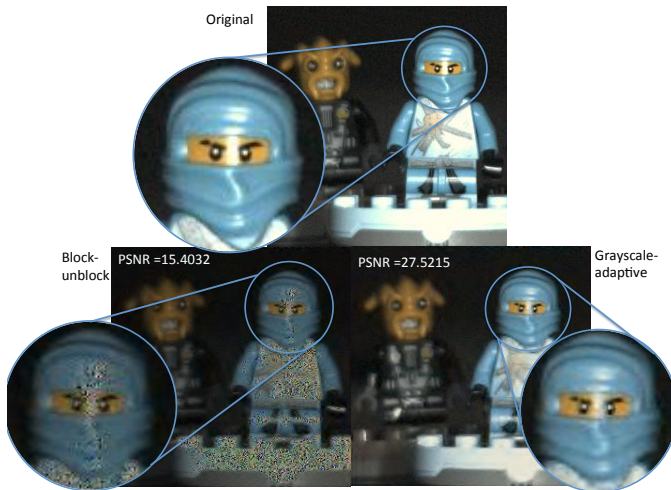


Fig. 7: Original and reconstructed images for block-unblock and grayscale-adaptive coded apertures. The zoomed images present a detail for the head of the object, (top) original and (bottom-left) the reconstructed image with block-unblock attaining 15.4032 dB, (bottom-right) grayscale-adaptive attaining 27.5215 dB. All reconstructions were obtained from FPA measurements with 10% of saturated pixels.

V. CONCLUSION

Grayscale adaptive coded apertures have been introduced in compressive spectral imaging system CASSI to replace the traditional block-unblock coded apertures. The proposed architecture permits to attenuate the effects of the saturation on the FPA sensors. The designed grayscale coded apertures outperform the block-unblock coded apertures in up to 12 dB in the quality of the reconstructed images. The percentage of saturation is corrected with grayscale adaptive coded apertures, while block-unblock coded apertures are unable to do so.

REFERENCES

[1] A. A. Wagadarikar, R. John, R. Willet, and D. Brady, "Single disperser design for coded aperture snapshot spectral imaging", *Appl. Opt.* 47, pp. B44-B51, 2008.

[2] E. J. Candes. "Compressive sampling", *Proceedings of the International Congress of Mathematics*, vol. 3, pp. 1433-1452, 2006.

[3] D. Donoho, "Compressed sensing", *IEEE Transactions on Information Theory*, vol. 52, pp. 1289-1306, 2006.

[4] R. Baraniuk. "Compressive sensing", *IEEE Signal Processing Magazine*, vol. 24, pp. 118-121, 2007.

[5] H. Arguello, P. Ye, and G. R. Arce, "Spectral aperture code design for multi-shot compressive spectral imaging", in *Digital Holography and Three-Dimensional Imaging, OSA Technical Digest (CD) (Optical Society of America, 2010)*.

[6] H. Arguello and G. R. Arce, "Code aperture design for compressive spectral imaging", in *European Signal Processing Conference, EUSIPCO (European Association for Signal Processing, 2010)*.

[7] H. Arguello and G. R. Arce, "Code aperture optimization for spectrally agile compressive imaging", *J. Opt. Soc. Am.*, vol. 28, pp. 2400-2413, 2011.

[8] H. Arguello and G. R. Arce, "Code aperture agile spectral imaging (CAASI)", *Imaging Systems Applications, OSA Technical Digest (CD) Optical Society of America, 2011*.

[9] D. Kittle and K. Choi and A. Wagadarikar and D. J. Brady, "Multiframe image estimation for coded aperture snapshot spectral imagers", *Appl. Opt.*, vol. 49, no. 36, pp. 6824-6833, 2010.

[10] Y. Wu, I. O. Mirza, G. R. Arce and D. W. Prather. "Development of a digital-micromirror-device-based multishot snapshot spectral imaging system", *emph. Opt., Lett.*, vol. 36, no. 14, pp. 2692-2694, 2011.

[11] H. Rueda, A. Calderon, H. Fuentes. "Spectral selectivity in compressive spectral imaging based on grayscale coded apertures", *Image, Signal Processing, and Artificial Vision (STSIVA), 2013 XVIII Symposium of*, pp. 1-5, 2013.

[12] J. N. Laska, P. T. Boufounos, M. A. Davenport, and Richard G. Baraniuk, "Democracy in action: Quantization, saturation, and compressive sensing", vol. 31, no. 3, pp. 429-443, 2011.

[13] M.A.T., Figueiredo, R.D., Nowak, and S.J., Wright. "Gradient Projection for Sparse Reconstruction: Application to Compressed Sensing and Other Inverse Problems", *IEEE Journal of Selected Topics in Signal Processing.*, vol. 4(1), 2007.

[14] S., Kitic, L. Jacques, N. Madhu, M.P. Hopwood, A. Spriet, C., De Vleeschouwer. "Consistent iterative hard thresholding for signal declipping", *Acoustics, Speech and Signal Processing (ICASSP), 2013 IEEE International Conference on*, pp. 5939-5943, 2013.

[15] S., Kitic, N. Bertin, and R. Gribonval. "Audio Declipping by Cospase Hard Thresholding, 2013.